

Short Communication

Determining the von Mises stress power spectral density for frequency domain fatigue analysis including out-of-phase stress components

M.H.A. Bonte^{a,*}, A. de Boer^a, R. Liebrechts^b

^aDepartment of Applied Mechanics, University of Twente, Drienerlolaan 5, Postbus 217, NL-7500 AE, Enschede, The Netherlands

^bDepartment Technical Analysis, DAF Trucks N.V., Hugo van der Goeslaan 1, Postbus 90065, NL-5600 PT, Eindhoven, The Netherlands

Received 3 October 2005; received in revised form 12 October 2006; accepted 13 November 2006

Available online 23 January 2007

Abstract

This paper provides a new formula to take into account phase differences in the determination of an equivalent von Mises stress power spectral density (PSD) from multiple random inputs. The obtained von Mises PSD can subsequently be used for fatigue analysis. The formula was derived for use in the commercial vehicle business and was implemented in combination with Finite Element software to predict and analyse fatigue failure in the frequency domain.

© 2007 Elsevier Ltd. All rights reserved.

1. Introduction

Mechanical fatigue is of major importance in the development of dynamically loaded structures. Performing numerical analyses to predict fatigue helps to shorten development time and cost.

High-cycle fatigue can be analysed by means of the so-called stress-life approach [1]. Using this method, fatigue failure prediction is based on the magnitude and mean of the stresses occurring in the construction. The stress amplitude and the mean stress caused by the loading can be rainflow counted and related to an $S-N$ curve, which gives the number of cycles that can be applied to the structure until failure [2]. The total fatigue damage may be determined by using the Palmgren–Miner rule. $S-N$ curves are usually determined for uni-axial stress states.

However, in a real environment, stresses will not be uni-axial, but bi-axial or in the most general case multi-axial. Many multi-axial fatigue criteria have been developed (see e.g. Refs. [3,4]). Many of them are based on the critical plane approach. Alternatively, it is possible to calculate an equivalent stress from the multi-axial stresses, which can subsequently be used to perform uni-axial stress-life fatigue analysis as described above. Popular equivalent stresses are the von Mises stress, the maximum principal stress and the maximum shear stress (Tresca).

*Corresponding author.

E-mail address: m.h.a.bonte@utwente.nl (M.H.A. Bonte).

Fatigue analyses are mostly performed in the time domain, in which equivalent dynamic stresses can be easily calculated and the stress-life method introduced above can be applied without further problems. However, if the vibrations in a construction have a random character, fatigue analysis is often based on multi-axial stress power spectral densities (PSDs) in the frequency domain. Calculating an equivalent stress from these stress PSDs and performing frequency domain fatigue analysis is less trivial. Several authors have introduced methods to calculate equivalent stresses in the frequency domain [5–10].

In this paper, we are considering Preumont and Piémont's very useful stress-life fatigue analysis procedure [5]. It will be shown that Preumont's method does not take into account phase differences between the multi-axial stress components while calculating an equivalent von Mises stress PSD. However, these phase differences can be present in real life in case of multiple random excitations, e.g. road excitation for trucks. A new formula will be derived that includes phase differences between the multi-axial stress PSDs.

As a basis, Section 2 shortly describes the appearance of the multi-axial stress PSDs from which we would like to calculate an equivalent stress PSD. We apply the von Mises stress as an equivalent stress. The calculation of the von Mises stress in the time-domain is reviewed in Section 3. In Section 4, it is shown that Preumont's formula does not take into account phase differences. The new formula that takes into account phase differences is derived in Section 5. In Section 6, it is shortly indicated how the new formula can be included in frequency domain stress-life fatigue analysis. An automotive example case comparing both Preumont's and the new formula is also included in Section 6.

2. Determination of the bi-axial stress responses from multiple random excitations

Assume a structure that is dynamically loaded by multiple random excitations, e.g. a truck loaded by road irregularities through its wheels. In this case, the random road excitation of the i th wheel of a truck is given by $\mathbf{G}_{ii}(f)$, the Fourier transform of the auto correlation function of the excitation signal. This is called the PSD.

Correlations that exist between the wheels are taken into account using cross PSDs. Wheels at the left rear of a truck are subjected to the same excitation as the left front wheel, only after a time delay, i.e. a phase difference is present in the cross PSDs between front and rear wheels. This phase difference results in complex cross PSDs. Similar correlations exist between left and right wheels.

For each frequency f_m , the input PSD matrix $\mathbf{G}(f_m)$ can now be defined as

$$\mathbf{G}(f_m) = \begin{bmatrix} G_{11}(f_m) & \cdots & G_{1n}(f_m) \\ \vdots & \ddots & \vdots \\ G_{1n}^*(f_m) & \cdots & G_{nn}(f_m) \end{bmatrix} \quad (1)$$

in which $G_{1n}^*(f_m)$ denotes the complex conjugate of $G_{1n}(f_m)$. Eq. (1) is a Hermitic matrix, containing the auto PSDs on the diagonal and the cross PSDs on the off-diagonal positions. The size of the matrix is $n \times n$, with n the number of multiple excitations. For a truck with 12 wheels $\mathbf{G}(f_m)$ is a 12×12 matrix. A more detailed description of the construction of the input PSD matrix for trucks excited by road irregularities is presented by Anderson [11].

The response stress PSDs can now be determined from this excitation PSD matrix using a matrix of transfer functions $\mathbf{H}_\sigma(f_m)$ [12]:

$$\mathbf{G}_{\sigma\sigma}(f_m) = \mathbf{H}_\sigma^*(f_m) \cdot \mathbf{G}(f_m) \cdot \mathbf{H}_\sigma^T(f_m). \quad (2)$$

In case of multi-axial stresses, the stress response PSD matrix $\mathbf{G}_{\sigma\sigma}(f_m)$ is a 6×6 matrix. For fatigue, however, it is often assumed that cracks start at a free surface where a bi-axial stress state exists [2], in which case $\mathbf{G}_{\sigma\sigma}(f_m)$ reduces to a 3×3 matrix. This is also the case when analysing thin plates. Two normal (in x - and y -direction) and one shear stress (in the xy -plane) PSD remain:

$$\mathbf{G}_{\sigma\sigma}(f_m) = \begin{bmatrix} G_{\sigma_{xx},\sigma_{xx}} & G_{\sigma_{xx},\sigma_{yy}} & G_{\sigma_{xx},\tau_{xy}} \\ G_{\sigma_{xx},\sigma_{yy}}^* & G_{\sigma_{yy},\sigma_{yy}} & G_{\sigma_{yy},\tau_{xy}} \\ G_{\sigma_{xx},\tau_{xy}}^* & G_{\sigma_{yy},\tau_{xy}}^* & G_{\tau_{xy},\tau_{xy}} \end{bmatrix} = \begin{bmatrix} E(\sigma_{xx}^* \sigma_{xx}) & E(\sigma_{xx}^* \sigma_{yy}) & E(\sigma_{xx}^* \tau_{xy}) \\ E(\sigma_{xx} \sigma_{yy}^*) & E(\sigma_{yy}^* \sigma_{yy}) & E(\sigma_{yy}^* \tau_{xy}) \\ E(\sigma_{xx} \tau_{xy}^*) & E(\sigma_{yy} \tau_{xy}^*) & E(\tau_{xy}^* \tau_{xy}) \end{bmatrix} \quad (3)$$

with E the expected value operator.

3. The von Mises stress in the time domain

For uni-axial fatigue analysis, it is necessary to determine an equivalent stress from the bi-axial stress state. We use the von Mises stress σ_{VM} , which can be calculated in the time domain by

$$\sigma_{VM}^2(t) = \sigma_{xx}^2(t) + \sigma_{yy}^2(t) - \sigma_{xx}(t)\sigma_{yy}(t) + 3\tau_{xy}^2(t). \tag{4}$$

Assuming sinusoidal stresses with zero mean stress but including phase differences, one inserts stresses of the form $\sigma(t) = \hat{\sigma} \cos(\omega t + \varphi)$ in Eq. (4) and calculates the von Mises equivalent stress by

$$\sigma_{VM}^2(t) = \text{Re}(\boldsymbol{\sigma})^T \mathbf{A} \text{Re}(\boldsymbol{\sigma}), \tag{5}$$

where

$$\text{Re}(\boldsymbol{\sigma}) = \left\{ \begin{array}{l} \hat{\sigma}_{xx} \cos(\omega t + \varphi_{xx}) \\ \hat{\sigma}_{yy} \cos(\omega t + \varphi_{yy}) \\ \hat{\tau}_{xy} \cos(\omega t + \varphi_{xy}) \end{array} \right\} \text{ and } \mathbf{A} = \begin{bmatrix} 1 & -0.5 & 0 \\ -0.5 & 1 & 0 \\ 0 & 0 & 3 \end{bmatrix}.$$

Fig. 1(a) presents the equivalent time domain von Mises stress for the general case of out-of-phase bi-axial stresses. $\boldsymbol{\sigma}$ in Eq. (5) is the complex and time-dependent bi-axial stress vector. Eq. (5) can be rewritten to

$$\sigma_{VM}^2(t) = \text{Re}(\boldsymbol{\sigma})^T \mathbf{A} \text{Re}(\boldsymbol{\sigma}) = \left(\frac{\boldsymbol{\sigma}^T + \boldsymbol{\sigma}^H}{2} \right) \mathbf{A} \left(\frac{\boldsymbol{\sigma} + \boldsymbol{\sigma}^*}{2} \right) = \frac{\boldsymbol{\sigma}^H \mathbf{A} \boldsymbol{\sigma} + \text{Re}(\boldsymbol{\sigma}^T \mathbf{A} \boldsymbol{\sigma})}{2}. \tag{6}$$

$\boldsymbol{\sigma}^*$ is a vector containing the complex conjugates of the complex bi-axial stresses and $\boldsymbol{\sigma}^H$ denotes the Hermitian conjugate of the complex stress vector. In the complex plane, Eq. (6) may be displayed as a vector of length $\text{abs}(0.5(\boldsymbol{\sigma}^T \mathbf{A} \boldsymbol{\sigma}))$ rotating with time around the point $0.5(\boldsymbol{\sigma}^H \mathbf{A} \boldsymbol{\sigma})$ as shown in Fig. 1(b).

4. The von Mises stress PSD neglecting phase differences

In 1994, Preumont and Piéfort [5] proposed the following formula for the calculation of an equivalent stress PSD based on the von Mises stress:

$$\begin{aligned} G_{\sigma VM}(f_m) &= \text{trace}(\mathbf{A} \cdot \mathbf{G}_{\sigma\sigma}(f_m)) \\ &= G_{\sigma_{xx},\sigma_{xx}}(f_m) - \text{Re}(G_{\sigma_{xx},\sigma_{yy}}(f_m)) + G_{\sigma_{yy},\sigma_{yy}}(f_m) + 3G_{\tau_{xy},\tau_{xy}}(f_m) \end{aligned} \tag{7}$$

in which $\mathbf{G}_{\sigma\sigma}(f_m)$ denotes the multi-axial stress PSD matrix from Eq. (3).

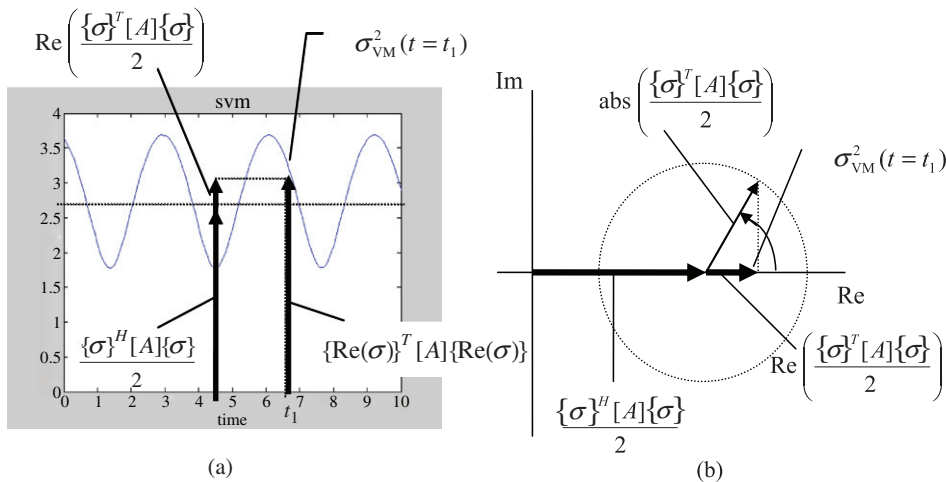


Fig. 1. (a) Time domain von Mises stress for out-of-phase bi-axial stresses; and (b) The von Mises stress as a rotating vector in the complex plane.

The auto PSD values at frequency band f_m are equivalent to the amplitudes of the sinusoidal stress-time domain signals:

$$G_{\sigma_{xx},\sigma_{xx}} = E(\sigma_{xx}^* \sigma_{xx}) \sim \hat{\sigma}_{xx}^2.$$

The cross PSD values at certain frequency f_m are equivalent to the following expression:

$$G_{\sigma_{xx},\sigma_{yy}} = E(\sigma_{xx}^* \sigma_{yy}) \sim \hat{\sigma}_{xx} \hat{\sigma}_{yy} \cos(\varphi_{xx} - \varphi_{yy}).$$

We can now write Eq. (7) as

$$G_{\sigma_{VM}}(f_m) = \hat{\sigma}_{xx}^2 - \hat{\sigma}_{xx} \hat{\sigma}_{yy} \cos(\varphi_{xx} - \varphi_{yy}) + \hat{\sigma}_{yy}^2 + 3\hat{\tau}_{xy}^2 = \boldsymbol{\sigma}^H \mathbf{A} \boldsymbol{\sigma} \tag{8}$$

with

$$\boldsymbol{\sigma} = \begin{Bmatrix} \hat{\sigma}_{xx} e^{j(\omega t + \varphi_{xx})} \\ \hat{\sigma}_{yy} e^{j(\omega t + \varphi_{yy})} \\ \hat{\tau}_{xy} e^{j(\omega t + \varphi_{xy})} \end{Bmatrix}.$$

Since Eq. (8) neglects phase differences between the bi-axial stresses, it is always larger than Eq. (6). Only in case the stresses are in-phase, it yields the same results. This can also be observed in Fig. 1(b).

Fig. 2(a) presents a time domain von Mises stress which was calculated from in-phase bi-axial stresses by Eq. (4). The result of Eq. (7) for the same in-phase bi-axial stresses described in the frequency domain is indicated in Fig. 2(a) as the dashed line. Thus, Fig. 2(a) shows that in case of in-phase bi-axial stresses, Eq. (7) exactly calculates the maximum value of the corresponding time-dependent von Mises stress. This maximum von Mises stress can subsequently be used for further uni-axial fatigue analysis. Thus, Eq. (7) is valid in case of in-phase bi-axial stresses. For out-of-phase bi-axial stresses, however, Fig. 2(b) shows that Eq. (7) overestimates the maximum von Mises stress.

5. A new formula for the von Mises stress PSD including phase differences

We will now propose a new formula that includes phase differences. We assume zero mean bi-axial stresses including phase differences as introduced in Eq. (5) in Section 3. Using the goniometric relationship

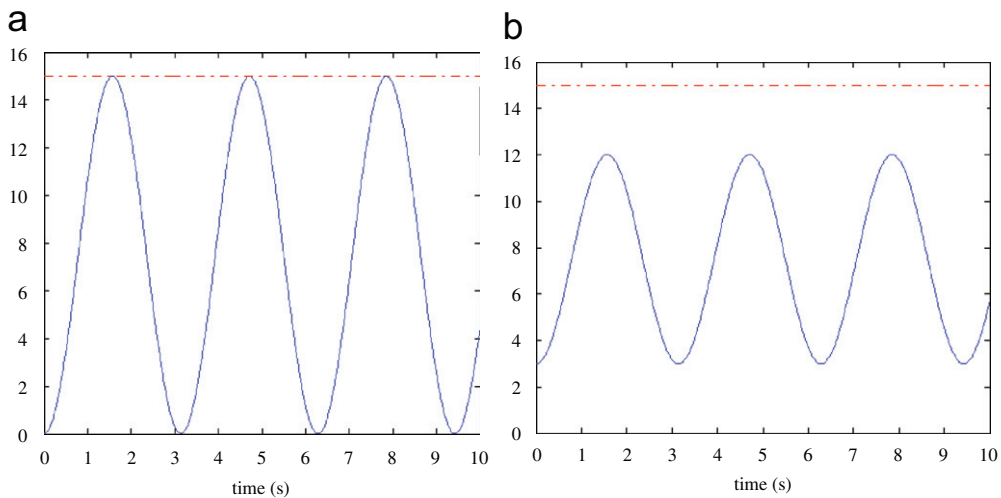


Fig. 2. (a) In-phase bi-axial stresses: time-dependent von Mises stress (solid line) and PSD value calculated using Eq. (7) (dashed line); and (b) out-of-phase bi-axial stresses: time-dependent von Mises stress (solid line) and PSD value calculated using Eq. (7) (dashed line).

$\cos^2(\omega t + \varphi) = 0.5(1 + \text{Re}(e^{2j(\omega t + \varphi)}))$, Eq. (5) can be rewritten to

$$\sigma_{\text{VM}}^2(t) = 0.5(\hat{\sigma}_{xx}^2 + \hat{\sigma}_{yy}^2 + 3\hat{\tau}_{xy}^2) + 0.5\left(\hat{\sigma}_{xx}^2 \text{Re}(e^{2j(\omega t + \varphi_{xx})}) + \hat{\sigma}_{yy}^2 \text{Re}(e^{2j(\omega t + \varphi_{yy})}) + 3\hat{\tau}_{xy}^2 \text{Re}(e^{2j(\omega t + \varphi_{xy})})\right) - \text{Re}(\hat{\sigma}_{xx} e^{j(\omega t + \varphi_{xx})}) \text{Re}(\hat{\sigma}_{yy} e^{j(\omega t + \varphi_{yy})}).$$

The last term of this equation may be deduced as follows:

$$\begin{aligned} \text{Re}(\hat{\sigma}_{xx} e^{j(\omega t + \varphi_{xx})}) \text{Re}(\hat{\sigma}_{yy} e^{j(\omega t + \varphi_{yy})}) &= \left(\frac{\hat{\sigma}_{xx} e^{j(\omega t + \varphi_{xx})} + \hat{\sigma}_{xx} e^{-j(\omega t + \varphi_{xx})}}{2}\right) \left(\frac{\hat{\sigma}_{yy} e^{j(\omega t + \varphi_{yy})} + \hat{\sigma}_{yy} e^{-j(\omega t + \varphi_{yy})}}{2}\right) \\ &= 0.5\hat{\sigma}_{xx}\hat{\sigma}_{yy} \text{Re}(e^{2j\omega t} e^{j(\varphi_{xx} + \varphi_{yy})}) + 0.5\hat{\sigma}_{xx}\hat{\sigma}_{yy} \cos(\varphi_{xx} - \varphi_{yy}). \end{aligned}$$

The von Mises stress now becomes

$$\begin{aligned} \sigma_{\text{VM}}^2(t) &= 0.5\left(\hat{\sigma}_{xx}^2 + \hat{\sigma}_{yy}^2 - \hat{\sigma}_{xx}\hat{\sigma}_{yy} \cos(\varphi_{xx} - \varphi_{yy}) + 3\hat{\tau}_{xy}^2\right) \\ &\quad + 0.5\text{Re}\left(\left(\hat{\sigma}_{xx}^2 e^{2j\varphi_{xx}} + \hat{\sigma}_{yy}^2 e^{2j\varphi_{yy}} - \hat{\sigma}_{xx}\hat{\sigma}_{yy} e^{j(\varphi_{xx} + \varphi_{yy})} + 3\hat{\tau}_{xy}^2 e^{2j\varphi_{xy}}\right) e^{2j\omega t}\right). \end{aligned}$$

Note the resemblance with Fig. 1(b). The first part is the mean of the von Mises stress, the second part is the real part of the vector rotating with time. As indicated in Section 4, the interesting stress quantity to take into account for fatigue analysis is the maximum von Mises stress. Calling to mind the zero mean bi-axial stress assumption, this maximum von Mises stress equals the von Mises mean plus the modulus of the rotating vector:

$$\begin{aligned} \max(\sigma_{\text{VM}}^2) &= 0.5\left(\hat{\sigma}_{xx}^2 + \hat{\sigma}_{yy}^2 - \hat{\sigma}_{xx}\hat{\sigma}_{yy} \cos(\varphi_{xx} - \varphi_{yy}) + 3\hat{\tau}_{xy}^2\right) \\ &\quad + 0.5\text{abs}\left(\hat{\sigma}_{xx}^2 e^{2j\varphi_{xx}} + \hat{\sigma}_{yy}^2 e^{2j\varphi_{yy}} - \hat{\sigma}_{xx}\hat{\sigma}_{yy} e^{j(\varphi_{xx} + \varphi_{yy})} + 3\hat{\tau}_{xy}^2 e^{2j\varphi_{xy}}\right) \\ &= 0.5\left(\hat{\sigma}_{xx}^2 + \hat{\sigma}_{yy}^2 - \hat{\sigma}_{xx}\hat{\sigma}_{yy} \cos(\varphi_{xx} - \varphi_{yy}) + 3\hat{\tau}_{xy}^2\right) \\ &\quad + 0.5\text{abs}\left(\hat{\sigma}_{xx}^2 + \hat{\sigma}_{yy}^2 e^{2j(\varphi_{yy} - \varphi_{xx})} - \hat{\sigma}_{xx}\hat{\sigma}_{yy} e^{j(\varphi_{yy} - \varphi_{xx})} + 3\hat{\tau}_{xy}^2 e^{2j(\varphi_{xy} - \varphi_{xx})}\right). \end{aligned}$$

For each frequency f_m , the von Mises PSD value is defined as the maximum von Mises stress, which results in the following alternative for Eq. (7):

$$\begin{aligned} G_{\sigma\text{VM}}(f_m) &= 0.5\left(\hat{\sigma}_{xx}^2 + \hat{\sigma}_{yy}^2 - \hat{\sigma}_{xx}\hat{\sigma}_{yy} \cos(\varphi_{xx} - \varphi_{yy}) + 3\hat{\tau}_{xy}^2\right) \\ &\quad + 0.5\text{abs}\left(\hat{\sigma}_{xx}^2 + \hat{\sigma}_{yy}^2 e^{2j(\varphi_{yy} - \varphi_{xx})} - \hat{\sigma}_{xx}\hat{\sigma}_{yy} e^{j(\varphi_{yy} - \varphi_{xx})} + 3\hat{\tau}_{xy}^2 e^{2j(\varphi_{xy} - \varphi_{xx})}\right). \end{aligned} \tag{9}$$

All amplitude terms in Eq. (9) can be derived from the response stress PSDs of $\mathbf{G}_{\sigma\sigma}(f_m)$ as defined in Eq. (3):

$$\begin{aligned} \hat{\sigma}_{xx}^2(f_m) &= \sigma_{xx}^*(f_m)\sigma_{xx}(f_m) = G_{\sigma_{xx},\sigma_{xx}}(f_m), \quad \hat{\sigma}_{yy}^2(f_m) = G_{\sigma_{yy},\sigma_{yy}}(f_m), \quad \hat{\tau}_{xy}^2(f_m) = G_{\tau_{xy},\tau_{xy}}(f_m), \\ \hat{\sigma}_{xx}(f_m)\hat{\sigma}_{yy}(f_m) &= \sqrt{\hat{\sigma}_{xx}^2(f_m)\hat{\sigma}_{yy}^2(f_m)} = \sqrt{G_{\sigma_{xx},\sigma_{xx}}(f_m)G_{\sigma_{yy},\sigma_{yy}}(f_m)}. \end{aligned}$$

For the phase angles the following relation can be derived:

$$\begin{aligned} \varphi_{yy}(f_m) - \varphi_{xx}(f_m) &= \text{angle}(G_{\sigma_{xx},\sigma_{yy}}(f_m)), \\ \varphi_{xy}(f_m) - \varphi_{xx}(f_m) &= \text{angle}(G_{\sigma_{xx},\tau_{xy}}(f_m)). \end{aligned}$$

For in-phase stresses, Eq. (9) reduces to Eq. (7). Fig. 3 shows that Eq. (9) indeed gives the maximum von Mises stress for both in-phase and out-of-phase bi-axial stresses. The formula can be extended to multi-axial stresses without further problems.

The formula has been derived for bi-axial stresses assuming a zero mean stress. Non-zero mean stresses could be incorporated using the first stress invariant of the static stress tensor and the Goodman diagram [5,8].

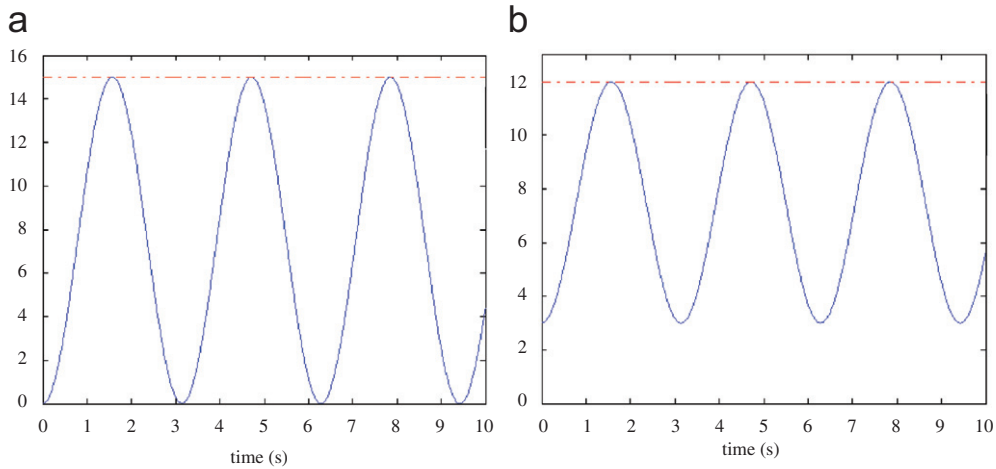


Fig. 3. (a) In-phase bi-axial stresses: time-dependent von Mises stress (solid line) and PSD value calculated using Eq. (9) (dashed line); and (b) out-of-phase bi-axial stresses: time-dependent von Mises stress (solid line) and PSD value calculated using Eq. (9) (dashed line).

6. Fatigue analysis of a truck chassis

The new formula can be included in frequency domain stress-life fatigue analysis as follows:

1. Calculate the response stress PSDs in each finite element using Eq. (2). The input PSD matrix of Eq. (1) should be known, the transfer functions $\mathbf{H}_\sigma(f_m)$ follow from a Finite Element frequency response analysis.
2. Calculate the von Mises equivalent stress using the new formula presented in Eq. (9).
3. Perform a Dirlik rainflow count [13,14] on the von Mises stress PSD.
4. Apply the Palmgren–Miner rule to determine the fatigue damage.

To demonstrate the above analysis, we will apply it to a small example. The above procedure and another example have also been demonstrated in another paper by the authors [15]. For this example, consider a truck driving over a specific road type at a speed of 50 km/h. The road surface information has been measured and is presented as a PSD. Using the truck's velocity and its wheelbase, one can determine the input PSD matrix $\mathbf{G}(f_m)$ of Eq. (1) from this road surface information PSD. NASTRAN Finite Element software is used to calculate the transfer functions $\mathbf{H}_\sigma(f_m)$. Eq. (2) yields the response stress PSDs in each finite element.

The next step is to determine the von Mises equivalent stress by the new formula (Eq. (9)). Fig. 4(a) presents the results for a part of the truck's chassis. Fig. 4(b) presents the results when Eq. (7) is applied instead of Eq. (9). One can observe different contours in the lower part of the chassis beam where out-of-phase stresses are known to be present. It can be seen that Eq. (9)—as expected—yields lower stress values in this region than Eq. (7). Fig. 5 shows for both formulas the von Mises stress PSDs in finite element X indicated in Fig. 4. Again the difference between Eq. (9) and Eq. (7) is clearly demonstrated. However, the considered element is not the hot-spot, which is located near the hole in the chassis beam (see Fig. 4). Here, stresses are close to uni-axial and the difference between both formulas diminishes.

The third and fourth step of the fatigue analysis comprise Dirlik rainflow counting [13–15] and applying the Palmgren–Miner rule to yield the expected fatigue damage. For both Eq. (9) and Eq. (7) Palmgren–Miner numbers have been calculated to be 78 975 and 93 814, respectively. Hence, the fatigue damage of element X is estimated to be 19% higher using Eq. (7) than using Eq. (9). It can be concluded from this example that using Eq. (9) instead of Eq. (7) results in a less conservative fatigue life estimate for certain locations in a construction where the multi-axial stresses are out-of-phase.

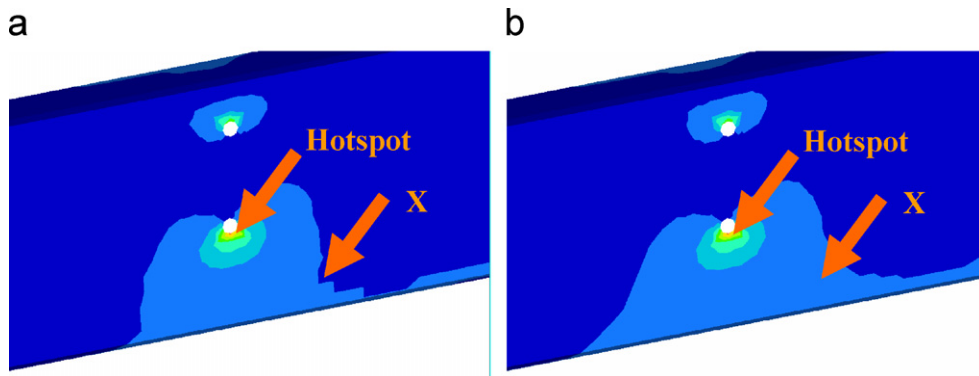


Fig. 4. (a) von Mises stress in a truck chassis calculated using the new formula Eq. (9); and (b) von Mises stress in a truck chassis using Preumont's formula Eq. (7).

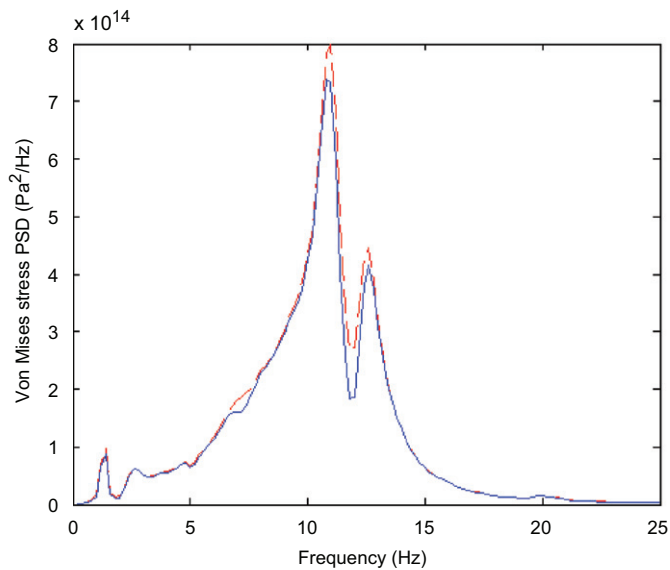


Fig. 5. von Mises stress PSD histogram in a truck chassis calculated using Eq. (7) (dashed line) and Eq. (9) (solid line).

7. Conclusions

A practical formula has been derived for determining an equivalent von Mises stress in the frequency domain. Assuming zero mean, sinusoidal multi-axial stresses, it takes into account phase differences between the multi-axial stress components. This calculated von Mises PSD can subsequently be used for frequency domain fatigue analysis of structures that are randomly excited by multiple loads, e.g. a truck subjected to road irregularities.

Acknowledgements

Acknowledged is DAF Trucks N.V. in Eindhoven, The Netherlands, who funded, facilitated and participated in the research project.

References

- [1] D.F. Socie, G.B. Marquis, *Multiaxial Fatigue*, Society of Automotive Engineers, Warrendale, PA, USA, 2000.
- [2] D. Radaj, *Ermüdungsfestigkeit*, Springer, Berlin, Germany, 1995 (in German).
- [3] Y.Y. Wang, W.X. Yao, Evaluation and comparison of several multiaxial fatigue criteria, *International Journal of Fatigue* 26 (2004) 17–25.
- [4] Y. Liu, S. Mahadevan, Multiaxial high-cycle fatigue criterion and life prediction for metals, *International Journal of Fatigue* 27 (2005) 790–800.
- [5] A. Preumont, V. Piéfort, Predicting random high-cycle fatigue life with finite elements, *Journal of Vibration and Acoustics* 116 (1994) 245–248.
- [6] D. Segalman, G. Reese, R. Field Jr., C. Fulcher, Estimating the probability distribution of von Mises stress for structures undergoing random excitation, *Journal of Vibration and Acoustics* 122 (1) (2000) 42–48.
- [7] A. Preumont, X. Pitoiset, Discussion: estimating the probability distribution of von Mises stress for structures undergoing random excitation, *Journal of Vibration and Acoustics* 122 (2000) 336.
- [8] X. Pitoiset, A. Preumont, Spectral methods for multi-axial random fatigue analysis of metallic structures, *International Journal of Fatigue* 22 (2000) 541–550.
- [9] X. Pitoiset, I. Rychlik, A. Preumont, Spectral methods to estimate local multiaxial fatigue failure for structures undergoing random vibrations, *Fatigue & Fracture of Engineering Materials & Structures* 24 (2001) 715–728.
- [10] T. Lagoda, E. Macha, A. Nieslony, Fatigue life calculation by means of the cycle counting and spectral methods under multiaxial random loading, *Fatigue & Fracture of Engineering Materials & Structures* 28 (2005) 409–420.
- [11] J.B. Anderson, *Frequency Domain Fatigue Analysis of Commercial Vehicles Based on a Modular Finite Element Library*, Society of Automotive Engineers (SAE), Warrendale, PA, USA, 2003.
- [12] L. Meirovitch, *Elements of Vibration Analysis*, second ed., McGraw-Hill Book Company, Singapore, 1986.
- [13] T. Dirlik, Application of Computers in Fatigue Analysis, PhD Thesis, University of Warwick, UK, 1985.
- [14] N.W.M Bishop, The Use of Frequency Domain Parameters to Predict Structural Fatigue, PhD Thesis, University of Warwick, UK, 1988.
- [15] M.H.A. Bonte, R. Liebrechts, A. De Boer, Prediction of mechanical fatigue caused by multiple random excitations, *Proceedings of the ISMA Conference*, Leuven, Belgium, 2004, pp. 697–708, ISBN:90-73802-82-2.